The novel proautophagy anticancer drug ABTL0812 potentiates chemotherapy in adenocarcinoma and squamous nonsmall cell lung cancer

Anna López-Plana[1,2,3], Patricia Fernández-Nogueira[1], Pau Muñoz-Guardiola[4,5], Sònia Solé-Sánchez[5], Elisabet Megías-Roda[4,5], Héctor Pérez-Montoyo[5], Patricia Jauregui[1], Marc Yeste-Velasco[5], Mariana Gómez-Ferreria[5], Tatiana Erazo[4], Elisabet Ametller[1], Leire Recalde-Percaz[1,2,3], Núria Moragas-Garcia[1], Aleix Noguera-Castells[6], Mario Mancino[1,2,3,6], Teresa Morán[7], Ernest Nadal[8], José Alfón[4], Carles Domènech[5], Pere Gascon[1,2,3,6,9], Jose M. Lizcano[4], Gemma Fuster[1,2,10,11] and Paloma Bragado[1,12]

[1]Molecular and Translational Oncology Group, Institut d'Investigacions Biomediques August Pi i Sunyer (IDIBAPS), Barcelona, Spain

[2]Biochemistry and Molecular Biomedicine Department, School of Biology, University of Barcelona, Barcelona, Spain

[3]Institut de Biomedicina de la Universitat de Barcelona (IBUB), University of Barcelona, Barcelona, Spain

[4]Protein Kinases and Signal Transduction Laboratory, Institut de Neurociències and Departament de Bioquímica i Biologia Molecular, Universitat Autònoma de Barcelona, Bellaterra, Barcelona, Spain

[5]Ability Pharmaceuticals, SL, Cerdanyola Del Vallès, Barcelona, Spain

[6]Department of Medicine, University of Barcelona, Barcelona, Spain

[7]Medical Oncology Department, Catalan Institute of Oncology - Badalona, Hospital Universitari Germans Trias i Pujol, Institut Germans Trias i Pujol, Badalona-Applied Research Group in Oncology, Universitat Autònoma de Barcelona, Barcelona, Spain

[8]Department of Medical Oncology, Thoracic Oncology Multidisciplinary Unit, Catalan Institute of Oncology, Barcelona, Spain

[9]Department of Medical Oncology, Hospital Clínic, Barcelona, Spain

[10]Department of Biochemistry & Physiology, School of Pharmacy and Food Sciences, University of Barcelona, Barcelona, Spain

[11]Department of Biosciences, Faculty of Sciences and Technology, University of Vic, Vic, Spain

[12]Department of Biochemistry and Molecular Biology, Faculty of Pharmacy, Complutense University of Madrid, Health Research Institute of the Hospital Clínico San Carlos, Madrid, Spain

A.L.-P., P.F.-N., G.F. and P.B. contributed equally to this work

Additional Supporting Information may be found in the online version of this article.

Key words: ABTL0812, lung cancer, chemoresistance autophagy, TRIB3

Abbreviations: AMPK: AMP-activated protein kinase; CCCP: carbonyl cyanide m-chlorophenyl hydrazine; Cis: cisplatin; DAB: 3,3^{0}-dia- minobenzidine; Doc: docetaxel; IC50: half maximal inhibitory concentration; IRS: immunoreactive score; LKB1: liver kinase B1; NSCLC: non- small cell lung carcinoma; ON: overnight; P/C: paclitaxel and carboplatin; PA: pepstatin-A; PAM: PI3K/Akt/mTOR; PBMCs: peripheral blood mononuclear cells; Pem: pemetrexed; PI: propidium iodide; PPARα and PPARγ: peroxisome proliferator activated receptor alpha and gamma; RIPA: radioimmunoprecipitation assay; RT: room temperature; RTK: receptor tyrosine kinases; SI: staining intensity; SOC: standard of care; TRIB3: tribbles-3 pseudokinase

DOI: 10.1002/ijc.32865

History: Received 14 May 2019; Accepted 16 Dec 2019; Online 14 Jan 2020

Correspondence to: Gemma Fuster, E-mail: gemmafuster@ub.edu; or Paloma Bragado, E-mail: pbragado@ucm.es

Around 40% of newly diagnosed lung cancer patients are Stage IV, where the improvement of survival and reduction of disease-related adverse events is the main goal for oncologists. In this scenario, we present preclinical evidence supporting the use of ABTL0812 in combination with chemotherapy for treating advanced and metastatic Nonsmall cell lung adenocarcinomas (NSCLC) and squamous carcinomas. ABTL0812 is a new chemical entity, currently in Phase 1b/2a clinical trial for advanced squamous NSCLC in combination with paclitaxel and carboplatin (P/C), after successfully completing the first-in- human trial where it showed an excellent safety profile and signs of efficacy. We show here that ABTL0812 inhibits Akt/mTOR axis by inducing the overexpression of TRIB3 and activating autophagy in lung squamous carcinoma cell lines. Furthermore, treatment with ABTL0812 also induces AMPK activation and ROS accumulation. Moreover, combination of ABTL0812 with chemotherapy markedly increases the therapeutic effect of chemotherapy without increasing toxicity. We further show that combination of ABTL0812 and chemotherapy induces nonapoptotic cell death mediated by TRIB3 activation and autophagy induction. We also present preliminary clinical data indicating that TRIB3 could serve as a potential novel pharmacodynamic biomarker to monitor ABTL0812 activity administered alone or in combination with chemotherapy in squamous NSCLC patients. The safety profile of ABTL0812 and its good synergy with chemotherapy potentiate the therapeutic potential of current lines of treatment based on chemotherapy regimens, arising as a promising option for improving these patients therapeutic expectancy.

What's new?

Non-small cell lung carcinoma is a common lung cancer with poor prognosis due to late diagnosis and frequent drug resistance of the tumor. Here the authors examined the cytotoxic effect of ABTL0812, a new AKT/mTOR inhibitor currently under clinical development, in combination with common chemotherapy regimens in lung squamous carcinoma cell lines. They demonstrate non-apoptotic cell death mediated by activation of the Tribbles-3 pseudokinase (TRIB3) and autophagy induction in response to ABTL0812 co-treatment, proposingTRIB3 as a potential new biomarker to monitor the activity of ABTL0812 treatment in human clinical trials.

INTRODUCTION

Lung cancer is one of the most aggressive cancers showing one of the highest death rates,[1,2] with a 17.8% 5-year survival rate and around 50% of deaths within the first year. It is esti- mated that 1.2 million new cases are diagnosed every year in most developed countries and it has become one of the lead- ing cancer deaths in western countries.[3]

Lung cancers are divided into two main types, small and nonsmall cell carcinomas. Nonsmall cell carcinomas (NSCLC) account for around 85% of total lung cancers and are further divided into squamous-cell carcinoma (25–30% of all lung cancers), large-cell carcinoma (5–10% of all lung cancers) and adenocarcinomas, which are the most frequent and comprise around 40% of all lung cancers.[4,5] Unfortunately, the majority (70%) of NSCLC are at an advanced stage at the time of diagnosis, limiting their chances of cure.

In resectable NSCLC patients with Stages I, II or IIIA, sur- gery is the best treatment option, either with or without adju- vant chemotherapy to treat micrometastatic disease and the only curative treatment. However, only 15–20% of tumors can be radically resected, leading to a 5-year survival rate of 40%.[6] For unresectable tumors, no single chemotherapy regime has shown a clear superiority in patients with locally advanced or metastatic NSCLC, and combination of two chemotherapy agents has been considered the standard of care for many years, although the toxicity associated to these treatments is high.[7,8] Even when immunotherapy has entered the clinical scenario in lung cancer,[9,10] platinum doublets might be con- sidered once the disease progress to such therapies.

For patients with Stage IV, advanced, metastatic or recur- rent NSCLC, platinum-based chemotherapy doublets, includ- ing cisplatin with either paclitaxel, gemcitabine or docetaxel,[11] as well as carboplatin with paclitaxel[12,13] have been the treat- ment combination of choice. Concretely, nonsquamous NSCLC adenocarcinomas have been preferentially treated with pemetrexed with cisplatin or carboplatin[14,15] while pacli- taxel and carboplatin have been one of the favored options for squamous metastatic NSCLC.[16]

Apart from toxicity-related events, one of the main imped- iments for the therapeutic success of chemotherapy has been the development of drug resistance. The PI3K/Akt/mTOR (PAM)

pathway is a prototypic survival pathway that is con- stitutively activated in many types of cancer and plays a criti- cal role in resistance to chemotherapy.[17,18] PAM pathway integrates signals from survival or growth factor through ligand-stimulated receptor tyrosine kinases (RTK) and regu- lates numerous cellular processes such as growth, prolifera- tion, cell cycle progression, autophagy, motility, adhesion and angiogenesis.[19] Since chemotherapy regimens are the main treatment for NSCLC, inhibiting the PAM pathway might be a therapeutic option to avoid resistance to chemotherapy and improve treatment outcomes.

ABTL0812 is a novel anticancer agent under clinical devel- opment with a unique mechanism of action, through which it inhibits Akt/mTOR axis finally leading to an autophagy- mediated cancer cell death.[20,21] ABTL0812 primary targets are the peroxisome proliferator-activated receptor alpha and gamma (PPARα and PPARγ).[21] The activation of PPARα/γ transcriptional activity by ABTL0812, induces the upregulation of Tribbles-3 pseudokinase (TRIB3), a negative regulator of Akt phosphorylation. By binding to Akt, TRIB3 impedes its phos- phorylation by upstream kinases PDK1 and mTORC2, leading to the inhibition of the Akt/mTOR axis and, as a consequence inducing autophagy-mediated cancer cell death.[21]

ABTL0812 completed a first-in-humans clinical trial, showing a high safety profile and signs of efficacy[22] (NCT02201823). The recommended Phase II dose was deter- mined, and together with previous efficacy data on animal models, allowed for the protocol approval by regulatory authorities of the current Phase 1b/2a trial, where it is admin- istered as first-line therapy in combination with paclitaxel and carboplatin for treating advanced squamous nonsmall cell lung cancer patients (NSCLC; NCT03366480).

An important part of recently diagnosed lung cancer patients is Stage IV, in which the main objective is to improve survival and reduce adverse events related to this disease. Considering this clinical challenge, we provide preclinical evi- dence that reinforces the use of ABTL0812 combined with chemotherapy drugs for the treatment of advanced NSCLC and metastatic adenocarcinomas.

MATERIALS AND METHODS

Cell lines and cultures

Human adenocarcinoma cell lines A549 (RRID:CVCL_0023) (ATCC) (KRAS mutant) and NCI-H1975 (RRID:CVCL_1511) (*PI3K* mutant and EGFR mutant) and squamous-cell carcinoma NCI-H520 (RRID:CVCL_1566) (wild type) and NCI-H157 (RRID:CVCL_0463; *PTEN* null, the NCI-H1975, NCI-H520 and NCI-H157 were provided by Dr Jordi Alcaraz) were cul- tured under a humidified atmosphere of 5% CO_2 at 37°C in RPMI Media 1640 (Gibco, Waltham, MA), supplemented with 10% fetal bovine serum (FBS, Gibco), 5% Glutamax (Gibco) and 5% Fungizone–penicillin–streptomycin mixture (Invitrogen). All human cell lines have been authenticated using STR profiling within the last 3 years and all the experiments were performed with mycoplasma free cells.

Cell viability studies

Cell Titer 96 Aqueous One Solution Cell Proliferation Assay Kit (Promega) was used according to the manufacturer's instructions. Briefly, for docetaxel studies, subconfluent cul- tures of adenocarcinoma lung cancer cells were incubated for 72 hr in the presence of an increasing concentration of ABTL0812 (0–200 μM), docetaxel (0–100 μM) or the combi- nation of increasing doses of docetaxel with ABTL0812 20 μM. For paclitaxel studies, subconfluent cultures of adeno- carcinoma and squamous lung cancer cell lines were incu- bated for 48 hr in the presence of an increasing concentration of paclitaxel (0–1 μM) or the combination of increasing doses of paclitaxel with sub-IC50 concentrations of ABTL0812 (5–30 μM). Plates were read on a microplate spectrophotome- ter (Molecular Dynamics) at 490 nm (test wavelength) and 690 nm (reference wavelength). Determination of half- maximal inhibitory concentration (IC50), curve fitting and statistical analysis were performed using Graph Pad Prism® 5.0 Software. Values of $p < 0.05$ were considered statistically significant.

Western blot

Cells were seeded in six-well plates and grown until 70–80% confluence, cultured in 0.5% serum media overnight and treated with the indicated drugs at the indicated time and dose. Frozen cell pellets were lysed with ice-cold radio- immunoprecipitation assay (RIPA) buffer (Tris–HCl 5 mM, pH 7.4, 1% NP-40, 0.25% Na deoxycholate, NaCl 150 mM, EDTA 1 mM, PMSF 1 mM, proteinase inhibitors, Na_3VO_4 1 mM and NaF 1 mM) for protein extraction. After centrifu- gation (13,000 rpm for 20 min at 4°C), supernatants con- taining the protein fraction were collected and quantified by PIERCE method (Thermo Scientific, Waltham, MA). Equal amounts of total protein for each sample were sepa- rated in a SDS-PAGE gel and electrophoretically transferred to polyvinylidene difluoride membranes, blocked with TTBS- milk 5% for 1 hr at room temperature and incubated over- night (ON; 4°C) with the corresponding primary antibody (summarized in Supporting Information Table S1). The fol- lowing day membranes were incubated for 1 hr at room tem- perature (RT) with horseradish peroxidase-conjugated secondary antibodies (summarized in Supporting Information Table S1). GAPDH, actin and tubulin were used as house- keeping controls.

Membrane chemiluminescence was detected after ECL incubation and image capture was performed with a Lumines- cent Image Analyzer (LAS4000 Imaging System, Fujifilm, Japan). Image Studio Lite software was used for densitometric quantification.

Annexin V/PI costaining

Subconfluence cells were seeded in cell culture dish 60 mm × 15 mm in 10% FBS-RPMI 1640 (Gibco) medium, and then treated with the indicated drugs (ABTL0812, docetaxel, pacli- taxel, cisplatin, pemetrexed) for the indicated time and dose. In all studies, apoptotic or/and nonapoptotic cell death were determined using Annexin-V-FLUOS/PI Staining Kit (eBiosciences, San Diego, CA) according to manufacturer's instructions. In brief, cells from the culture supernatant and also attached cells were collected and blocked using 1%BSA for 30 min and subsequently incubated with Annexin V-FITC solution and propidium iodide (PI) for 15 min at 4°C. The samples were analyzed by flow cytometry (Fortessa, BD Bio- sciences, San Jose, CA) and were quantified using FACSDiva software (BD Biosciences, San Jose, CA). The cells were classi- fied as follows: alive (Annexin−/PI−), early apoptotic (Annexin+/PI−), late apoptotic (Annexin+/PI+) and non- apoptotic cell death (Annexin−/PI+).

Experiments in mice

All *in vivo* experiments were approved by the institution's ethics commission's regulations, following the guidelines established by the regional authorities (Barcelona University and Autonomous University of Barcelona Animal Experimen- tation Ethics Committee, Catalonia, Spain).

Five-week-old female athymic nude Foxn 1nu nu/nu mice (Janvier and Envigo) were kept under specific pathogen-free conditions at constant ambient temperature (22–24°C) and humidity (30–50%). The mice had access to sterilized food and tap water *ad libitum*. After each experiment, the animals were anesthetized and euthanized in accordance with our institution's ethics commission's regulations.

A549 (5×10^6), H1975 (2×10^6) and H157 (2.5×10^6) lung cancer cells were injected subcutaneously in one flank per animal. When tumors reached 80–100 mm^3, mice were randomly distributed into treatment groups and administered the corresponding treatments for each experiment including ABTL0812, docetaxel (Doc), paclitaxel (P), carboplatin (C), cisplatin (Cis) and pemetrexed (Pem) (treatment conditions (summarized in Supporting Information Table S2). Combina- tion groups include ABTL0812 + Doc, ABTL0812 + C/P or ABTL0812 + Cis/Pem. Glycerol 1% solution or PBS was administered to the control group. Once treatment was fin- ished, mice were sacrificed and tumors were surgically recov- ered, measured, fixed in 4% paraformaldehyde (PFA, Sigma) and embedded in paraffin for further immunohistochemistry analysis (Supporting Information Materials and Methods). Tumor volumes were measured as (length × $width^2$)/2, twice a week and changes in tumor volume between groups were analyzed by ANOVA. Values of $p < 0.05$ were considered sta- tistically significant.

Clinical samples

Blood samples from nine squamous NSCLC human patients recruited in the Phase 1a/2b clinical trial (NCT03366480) were analyzed for the expression of TRIB3 by RT-qPCR. For more detail look at the Supporting Information Materials and Methods section. The trial was approved by the local ethics committees of the participating sites and by the Spanish Medi- cines Agency according to Real Decreto

223/2004. According to the protocol, the study complies with all regulatory require- ments, good clinical practice and the ethical principles of the latest revision of the Declaration of Helsinki as adopted by the World Medical Association. All subjects received written and verbal information regarding the study at a prior interview and signed an informed consent document.

Cellular ROS determination

A total of 5×10^5 cells were seeded on six-well plates and were allowed to adhere for 24 hr. After the indicated treat- ment, medium was removed, cells were washed with PBS and harvested by trypsinization. Then, cells were resuspended in PBS 20 μM 2^0,7^0-dichlorofluorescein diacetate reagent (DCFH- DA) that turns highly fluorescent upon oxidation. After 30 min incubation at 37°C, fluorescence was detected by flow cytometry (Ex 490/Em 520). Carbonyl cyanide m- chlorophenyl hydrazone (CCCP, mitochondrial uncoupling agent) was used as a positive control.

Generation of TRIB3 knockdown cell lines

A549 and H157 cell lines were transduced with either Control shRNA Lentiviral Particles-A (Santa Cruz; sc-108080) or TRB-3 shRNA (h) Lentiviral Particles (Santa Cruz, sc- 44426-V). Briefly, A549 and H157 were plated in 6 cm diame- ter dishes with fresh complete medium (DMEM with 10% w/v FBS). When cells had reached an 80–85% confluence the medium was removed, a retroviral-enriched supernatant was added, and cells were incubated at 37°C/5% CO_2. Polybrene was added (5 μg/ml) to enhance the efficacy of retroviral transduction. Then, 48 hr after, cells were treated with puromycin 2 μg/ml. Individual clones were collected and amplified and the genotype was verified.

Overexpression of TRIB3

A549 cells were transfected with a plasmid containing TRIB3 gene (pLKO vector) using lipofectamine 3000 following the manufacturer protocol. Then, 4 μg of plasmid were transfected using 16 μl of lipofectamine 3000 (1:4 ratio). Then, 48 hr after transfection gene expression and viability were assessed.

Data availability

All data will be available upon request.

RESULTS

ABTL0812 potentiates docetaxel antitumor activity in lung adenocarcinomas

ABTL0812 is a chemically modified lipid-derived small mole- cule that has shown antitumor activity in a wide range of can- cer cell lines.[20,21] We have previously shown that ABTL0812 is cytotoxic against A549 cells *in vitro* when administered alone. Here, we investigated the synergistic effect of combin- ing ABTL0812 with docetaxel. Adenocarcinoma A549 cells were incubated with increasing concentrations of ABTL0812, docetaxel or sub-IC50 concentrations of ABTL0812 (20 μM) combined with increasing concentrations of docetaxel. Cell viability was evaluated and the corresponding IC50s were cal- culated. As expected, both ABTL0812 and docetaxel inhibit A549 cell viability *in vitro* (Fig. 1*a*). Moreover, combination of sub-IC50 dose of ABTL0812 (20 μM) with docetaxel reduced A549 cells IC50 to docetaxel more than 50 times (Fig. 1*a*) suggesting that ABTL0812 and docetaxel have a synergistic effect.

To examine the potential impact of ABTL0812 on the effect of docetaxel on lung cancer cell viability, we cultured cells in the presence of ABTL0812, docetaxel or both for 48 hr and then analyzed apoptosis by flow cytometry. As shown in Figure 1*b*, the analysis of annexin V/PI costaining revealed that ABTL0812 induces high levels of nonapoptotic cell death and low levels of apoptosis, while docetaxel had very little effect on viability at the doses used (Fig. 1*b*).

When both drugs were administered together, the viability of cancer cells was markedly reduced, showing a potentiation of both ABTL0812 and docetaxel effects that were associated with an

increase in nonapoptotic cell death (Fig. 1*b*).

We have previously shown that ABTL0812 inhibits PI3K/ Akt/mTOR pathway leading to an autophagy-mediated cancer cell death.[20,21] We found that the combination of ABTL0812 and docetaxel also induces LC3 processing and TRIB3 up- regulation (Figs. 1*c* and 1*d*). Of note, docetaxel also induces TRIB3 expression in our models, as it has been reported in other cancer models.[23]

To test the efficacy of ABTL0812 in potentiating docetaxel anticancer effect *in vivo*, we implanted A549 human lung ade- nocarcinoma cells subcutaneously into immunosuppressed nude mice and treated them with ABTL0812, docetaxel or a combination of both. Our previous results have shown that ABTL0812 inhibits tumor progression with an efficacy similar to docetaxel.[21] Interestingly, when ABTL0812 is administered in combination with docetaxel, ABTL0812 potentiates the therapeutic effect of chemotherapy, showing the highest inhibition of tumor progression (Fig. 1*e* and Supporting Infor- mation Fig. S1*a*). Importantly, the analysis of body weight indicates that the combination therapy has no major toxic effects (Supporting Information Fig. S1*b*). In addition, analysis of phospho-AKT levels in the tumors showed a decrease in AKT activation in the tumors treated with the combination therapy compared to the ones treated with docetaxel alone (Supporting Information Fig. S1*c*). Furthermore, analysis of TRIB3 expression in the tumors showed that TRIB3 was upregulated in the tumors that received ABTL0812, alone or in combination with docetaxel (Fig. 1*f*).

Therefore, our results suggest that ABTL0812 potentiates docetaxel antitumor activity by inducing TRIB3 activation and autophagy.

ABTL0812 induces cell death, inhibits AKT/mTOR axis, upregulates TRIB3 and alters cell energy homeostasis in both squamous and lung adenocarcinomas

To characterize the effect of ABTL0812 in lung cancer, we investigated the cytotoxic effect of ABTL0812 on a panel of lung cancer cell lines of different origin including adenocarci- noma and squamous phenotype with different mutations in the PI3K/Akt/mTOR pathway, and further characterized its mechanism of action. To cover all relevant mutations, we included two adenocarcinoma cell lines, A549 cells (KRAS mutated) and H1975 cells (PI3K and EGFR-T790M mutated) and two squamous cell lines, H157 cells (PTEN null) and H520 cells (will type). ABTL0812 was effective in all evaluated lung cancer cell lines (Fig. 2*a*). Differences of potency were observed, being in general squamous cell lines more sensitive than adenocarcinoma (Figs. 2*a*–2*c*). In addition, mutations in PI3K/Akt/mTOR pathway seem to have a positive impact on the efficacy of the compound (Fig. 2*c*).

We have previously shown that ABTL0812 induces cell death by inhibiting the Akt/mTOR pathway through the upregulation of TRIB3 gene expression in KRAS mutated A549 lung adenocarcinoma model.[21] Therefore, we then explored the mechanisms of action of ABTL0812 in one adenocarcinoma cell line PI3K and EGFR-T790M mutated and in two squamous carcinoma cell lines. We found that upon ABTL0812 treatment all cell lines showed inhibited AKT activ- ity and induced TRIB3 overexpression (Figs. 2*d*–2*g*). Interest- ingly, squamous carcinoma cell lines, that were more sensitive to ABTL0812 in cell viability studies, induced higher levels of TRIB3 mRNA expression compared to adenocarcinoma cell lines (Fig. 2*g*).

Moreover, the treatment of lung cancer cell lines with ABTL0812 also induced LC3 processing and LC3-II accumu- lation (Figs. 2*d*–2*f*), suggesting that ABTL0812 induced autophagy. Furthermore, treatment of H157 and H1975 can- cer cells with a combination of the lysosomal protease inhibi- tors E64d and Pepstatin-A (PA) that blocks the final step of autolysosomal degradation and ABTL0812 resulted in an enhancement of LC3-II accumulation (Supporting Informa- tion Figs. S2*a* and S2*b*) suggesting that ABTL0812 induced dynamic autophagy.

Autophagy is a dynamic process that regulates metabolism and cellular homeostasis.[24] To analyze ABTL0812 role in cel- lular homeostasis we also evaluated the activation of AMPK, a central regulator of cellular energy homeostasis,[25] in response to ABTL0812 treatment (Fig. 2*d*–2*f* and Supporting Informa- tion Fig. S2*c*). Interestingly, ABTL0812 induced AMPK phos- phorylation in H157, H1975 and H520 cell lines (Figs. 2*d*–2*f*) but not in A549 cells (Supporting Information Fig. 2*c*). These results could be explained by the fact that A549 cell line natu- rally lacks LKB1.[26] Since our

results suggest that ABTL0812 can alter cell energy homeostasis by regulating autophagy and AMPK activation, we also tested whether treatment with ABTL0812 induced reactive oxygen species (ROS) accumula- tion (Fig. 2*h*). Interestingly, ABTL0812 induced an increase in cellular ROS after 6 hr in both NSLC cell lines (Fig. 2*h*).

Hence, our results showed that treatment with ABTL0812 upregulates TRIB3, alters the cell energy homeostasis by inducing autophagy, AMPK activation and ROS accumulation and promotes cell death in both lung adenocarcinoma and squamous carcinoma cell lines.

ABTL0812 synergistically potentiates the cytotoxicity of paclitaxel in adenocarcinoma and squamous lung cancer cells by inducing nonapoptotic cell death

Given that in the clinical setting targeted therapies are often combined with chemotherapy, we studied the effect of combining ABTL0812 with paclitaxel on cell viability of ade- nocarcinoma and squamous lung cancer cells. Adenocarci- noma A549 and H1975, and squamous H157 and H520 cells were incubated with increasing concentrations of ABTL0812, paclitaxel or sub-IC50 concentrations of ABTL0812 (5–30 Mm cell line dependent) combined with increasing concentrations of paclitaxel.

Cell viability was evaluated in all cases by MTT assay (Fig. 3*a*) and the corresponding IC50s were calculated (Supporting Information Fig. 3*a*). As expected, ABTL0812 and paclitaxel were cytotoxic when used independently. The addition of a low concentration of ABTL0812, markedly increased paclitaxel cytotoxicity (Fig. 3*a* and Supporting Infor- mation Fig. S3*a*). Then, the potential synergism of ABTL0812 with paclitaxel was calculated according to the method of Chou and Talalay.[27,28] The combination of both drugs was synergistic in the full range of concentrations (Supporting Information Tables S3–S6).

Since we have previously shown that ABTL0812 inhibits Akt activation in all cell lines (Figs. 2*d*–2*f*), we compared the efficacy of ABTL0812 with an mTOR direct inhibitor (everolimus),[29] by comparing the synergy of both drugs with paclitaxel (Supporting Information Fig. S3*b*). Everolimus does not show synergy with paclitaxel (Supporting Informa- tion Fig. S3*b*) as ABTL0812 does (Fig. 3*a*), except in the case of H520 cells (wild type for PI3K/Akt/mTOR mutations), where it sensitizes cells to paclitaxel, although at significantly lesser extent compared to ABTL0812. Interestingly, combina- tion of ABTL0812 with everolimus, further sensitize cells to paclitaxel (Supporting Information Fig. S3*c*). Our results sug- gest that ABTL0812 combination with paclitaxel is more effec- tive than other mTOR inhibitors such as everolimus.

Next, we investigated the type of cell death induced by the combination of ABTL0812 and paclitaxel. Adenocarcinoma A549 and H1975, and squamous H157 and H520 cells were incubated for 48 hr with either ABTL0812, paclitaxel or both and then cell death was analyzed by annexin V/PI assay using flow cytometry (Figs. 3*b*–3*e* and Supporting Informa- tion Fig. S4*a*). As expected, ABTL0812 induced principally nonapoptotic cell death in all cell lines, while paclitaxel- induced primarily apoptosis (Figs. 3*b*–3*e* and Supporting Information Fig. S4*a*). In all cell lines, the combination of ABTL0812 and paclitaxel had an additive effect and ABTL0812 potentiated paclitaxel cytotoxicity by inducing pri- marily nonapoptotic cell death (Figs. 3*b*–3*e* and Supporting Information Fig. S4*a*).

ABTL0812 chemosensitizes lung cancer cells through TRIB3 activation and autophagy induction

We then investigated the mechanism of action implicated in the cancer cell death induction mediated by ABTL0812 and paclitaxel combination. We have previously shown that ABTL0812 induces TRIB3 upregulation and LC3 processing (Figs. 2*d*–2*g*). Interestingly, treatment with paclitaxel only induced autophagy in H157 cells although it was able to acti- vate TRIB3 in H1975 and H157 cells (Fig. 4*a*) similar to doce- taxel in A549 cells (Fig. 1*c*), suggesting that chemotherapy can also modulate TRIB3 activity.[23] Moreover, we found that, independently of the phenotype or the PI3K pathway muta- tions, the combination of ABTL0812 and paclitaxel further upregulated TRIB3 mRNA and protein levels in all the cell lines (Figs. 4*a*–4*b*). In addition, LC3 processing was also increased with the combination treatment (Fig. 4*a*) suggesting that ABTL0812 potentiates the

chemotherapy effect through the induction of autophagy *via* TRIB3.

To investigate the role of TRIB3 in ABTL0812 autophagy and cell death induction we generated A549 and H157 TRIB3 knockdown cells (Supporting Information Figs. S5*a* and S5*b*). Our results showed that inhibition of TRIB3 decreased LC3 processing and LC3-II levels in both cell types (Supporting Information Fig. S5*b*) suggesting that TRIB3 regulates autophagy. Interestingly, TRIB3 knockdown cells are much less sensitive to ABTL0812 (Fig. 4*c*), which confirms our results that ABTL0812 induction of cell death is dependent on TRIB3 upregulation (Fig. 4*c*). Furthermore, the cytotoxic effect of paclitaxel and ABTL0812 combination is also par- tially mediated by TRIB3, although other mechanisms might also be involved since TRIB3 downregulation only partially reverse ABTL0812 and paclitaxel combination induction of cell death (Fig. 4*c*).

Interestingly, treatment with paclitaxel and ABTL0812 pro- motes ROS accumulation (Fig. 4*d*) suggesting that ABTL0812 and paclitaxel combination effect may be partially dependent on this accumulation of ROS.

To test that TRIB3 upregulation is able to induce cell death and autophagy, we transfected A549 cells with a TRIB3 vector (Fig. 4*e*) and analyzed LC3 processing and viability 48 hr after transfection. Interestingly, TRIB3 overexpression induces LC3 processing (Fig. 4*e*). Furthermore, as shown in Supporting Information Figure S5*c* TRIB3 upregulation decreases cell viabil- ity suggesting TRIB3 overexpression can induce cell death. To study the mechanism, we performed Annexin V/IP studies. Our results showed that TRIB3 upregulation induces nonapoptotic cell death (Fig. 4*f* and Supporting Information Fig. S5*d*). Hence, our results showed that ABTL0812 induction of autophagy and cell death is mediated *via* TRIB3 upregulation and that inhibi- tion of TRIB3 induces resistance to ABTL0812 and ABTL0812 and paclitaxel combination treatment.

To investigate ABTL0812 and paclitaxel induction of autophagy we preincubated H1975 and H157 cells with E64d+ PA, treated them with ABTL0812 plus paclitaxel and evalu- ated LC3-II expression by western blot (Supporting Informa- tion Figs. S5*e* and S5*f*). LC3-II levels were increased when cells were preincubated with E64d + PA, autophagy inhibitors and treated with ABTL0812 alone or with ABTL0812 plus paclitaxel which indicates that there is an induction of auto- phagic flux even in the combinatory treatment that seems to be mediated by ABTL0812. To further analyze the role of autophagy in ABTL0812 induction of cell death, we pretreated H1975 lung adenocarcinoma cell line with the autophagy inhibitor chloroquine that inhibits both fusion of autophagosome with lysosome and lysosomal protein degra- dation.[30] We then treated the cells with ABTL0812, paclitaxel or both and measure cell death by flow cytometry (Fig. 4*g*). As shown before, ABTL0812 induced nonapoptotic cell death and potentiates the cytotoxic effect of paclitaxel. Pretreatment with chloroquine reduces ABTL0812-induced nonapoptotic cell death to the same levels as controls and does not affect paclitaxel-induced cell death (Fig. 4*g*). Interestingly, chloro- quine was also able to reverse ABTL0812 and paclitaxel syner- gistic effect, suggesting that autophagy plays a central role in the potentiation of paclitaxel-mediated cytotoxicity mediated by ABTL0812 in lung cancer cells.

ABTL0812 enhanced carboplatin and paclitaxel antitumor activity both in adenocarcinomas and squamous lung xenografts

Carboplatin and paclitaxel combo is the chemotherapy of choice for a wide range of cancers, including lung cancer, where it is administered as a first-line therapy or as second line after targeted therapies have failed, as in the case of EGFR mutated lung cancer that have developed resistance to tyro- sine kinase inhibitors (TKIs).[31] We therefore evaluated the effect of combining ABTL0812 with this chemotherapy combo *in vivo* using a squamous (H157) and an adenocarcinoma (H1975) cell lines.

Our results in H157 derived xenograft indicates that ABTL0812 inhibits tumor progression with an efficacy similar to a high dose of carboplatin/paclitaxel in short-term, showing similar survival rates (Fig. 5*a*). However, the best effect in long-term stabilization is observed when ABTL0812 is com- bined with chemotherapy, significantly increasing survival and showing a 75% survival after 20 days of treatment compared to chemotherapy alone treatment that showed 0% survival (Fig. 5*a*). Mice body weight analysis indicates that the combi- nation therapy has no major toxic effects, as no decrease in body weight is observed (Supporting Information Fig. S6*a*). *Ex vivo* immunohistochemical analysis

of treated xenografts revealed an upregulated TRIB3 in tumors treated with ABTL0812. Surprisingly, TRIB3 was also overexpressed in tumors treated with chemotherapy only. However, TRIB3 levels were highest in the tumors derived from animals treated with ABTL0812 and carboplatin and paclitaxel (Fig. 5*b*). Furthermore, cell proliferation, measured using Ki67 marker, was also decreased by all the treatments, but especially with the combination of ABTL0812 and carboplatin and paclitaxel (Fig. 5*c*), while cell cycle arrest measured by p27 staining was increased upon ABTL0812 treatment (Fig. 5*d*) further demonstrating the potentiation of chemotherapy when administered in combination with ABTL0812.

We also tested the efficacy of the ABTL0812 combination with carboplatin and paclitaxel in an adenocarcinoma xenograft model implanted with H1975 cells. These cells harbor mutation in PI3KCA and EGFR, including the T790M mutation in EGFR that has been associated with TKI resistance. In these adenocarcinoma cells, ABTL0812 have a similar efficacy to chemotherapy alone in reducing tumor growth. However, combination of ABTL0812 with carboplatin and paclitaxel has a synergetic effect where the therapeutic efficacy of chemotherapy is potentiated by ABTL0812, showing the highest tumor growth inhibition *in vivo* (Fig. 5*e* and Supporting Information Fig. S6*b*). In this case, TRIB3 was also upregulated, especially in tumors treated with the combination of the three drugs (Fig. 5*f*) validating the increase on TRIB3 levels as a potential biomarker for ABTL0812 treatment.

TRIB3 as potential pharmacodynamic marker in patients treated with ABTL0812

Additionally, we evaluated the activity of ABTL0812 in all evaluable patients included in phase 1b/2a clinical trial (NCT03366480), by monitoring the levels of TRIB3 mRNA in total blood using RT-qPCR. The potential use of TRIB3 as a pharmacodynamic biomarker was previously tested in human PBMCs collected from healthy donors and incubated *in vitro* with ABTL0812,[21] where the increase in mRNA TRIB3 levels in response to ABTL0812 was validated. In the present work, we collected blood samples at different times from patients treated with 1,300 mg tid: basal level, 8 hr after the first dose of ABTL0812, 1 week after the first dose of ABTL0812 and 28 days after the first dose of ABTL0812 (and 3 weeks after having received the first cycle of chemotherapy in combination with ABTL0812). The number of samples varies from each time point due to the fact that some samples were not correctly taken and therefore not suitable for analysis. Our results indicate that ABTL0812 induces overexpression of TRIB3 mRNA levels in whole blood as soon as 8 hr and is maintained 1 week after the first administration. Moreover, this increase is sustained 28 days after starting the first dose of ABTL0812 and 3 weeks after having received the first paclitaxel/carboplatin (P/C) cycle (Fig. 5*g*).

These preliminary results confirm our mechanistic data in patients and suggest that TRIB3 can be considered as a potential pharmacodynamic biomarker for ABTL0812 in NSCLC patients treated with ABTL0812 alone and in combination with paclitaxel/carboplatin and further studies must be carried out to assess its ability to monitor ABTL0812 activity.

ABTL0812 potentiated cisplatin and pemetrexed antitumor activity *in vivo*

Different trials have reported that pemetrexed in combination with platinum (cisplatin, carboplatin or oxaliplatin) showed significant antitumor activity in advanced NSCLC, being one of the first-line treatments of choice for these patients based on their health status.[14,15] Therefore, we explore whether ABTL0812 can also boost the cytotoxic activity of cisplatin and pemetrexed both *in vitro* and *in vivo*.

Adenocarcinoma A549 cells were treated *in vitro* for 48 hr with either ABTL0812, cisplatin, pemetrexed, cisplatin combined with pemetrexed and ABTL0812 combined with cisplatin and pemetrexed, and cell death was evaluated by flow cytometry. As seen for ABTL0812 combined with paclitaxel, we found that cisplatin and pemetrexed induced apoptosis, whereas ABTL0812 mainly induced nonapoptotic cell death (Fig. 6*a*). We did not observe a synergistic effect between cisplatin and pemetrexed *in vitro* at the doses studied (Fig. 6*a*), however, their combination with

ABTL0812 promoted cell death and increased nonapoptotic cell death (Fig. 6*a*). Treat- ment with the combination of ABTL0812 and cisplatin and pemetrexed induced LC3 processing (Fig. 6*b*) and TRIB3 pro- tein and mRNA upregulation (Figs. 6*b* and 6*c*) suggesting that the combination effect was mediated through autophagy induction.

We then tested the effect *in vivo* of the triple combination, ABTL0812, pemetrexed and cisplatin *versus* cisplatin and pemetrexed combination. Interestingly our results showed that ABTL0812 potentiate the chemotherapy effect and the triple combination had a potent antitumor effect (Fig. 6*d*) and no cytotoxicity (Supporting Information Fig. S6*c*). Furthermore, *ex vivo* analysis of the tumors showed that TRIB3 was upregulated with ABTL0812 treatment (Fig. 6*e*) also in the tri- ple combination. Therefore, these results validated the poten- tial combination of ABTL0812 with this chemotherapy combo for treating lung adenocarcinoma patients.

DISCUSSION

Patients with nonsmall cell lung cancer (NSCLC) which are not suitable for surgical resection show a high mortality rate, due to the ineffectiveness of chemotherapy and the toxicity associated with this treatment.[32] Thus, there remains an urgent need for designing new efficacious drug combinations to combat this disease without increasing unwanted toxic side effects. In our study, we showed how the combination of ABTL0812, a novel TRIB3-mediated autophagy promoting anticancer agent in clinical development, with different che- motherapy regimens commonly used in first and second line in NSCLC patients, potentiates chemotherapy antitumor effect without increasing its toxicity. We further show that the anti- tumorigenic activity of ABTL0812 and chemotherapy combi- nation is mediated by TRIB3 expression upregulation and autophagy induction which leads to cancer cell death. Further- more, we propose that TRIB3 expression in whole blood could be used as novel pharmacodynamic biomarker for human patients with squamous NSCLC from Phase II trial treated with ABTL0812. Taken together, these results suggest that the therapeutic combination of ABTL0812 with chemotherapy is an attractive target for treating NSCLC.

In locally advanced or metastatic nonsquamous NSCLC the front line of systemic treatment used to include double treatment with a platinum agent such as cisplatin or car- boplatin, and a third-generation agent such as gemcitabine or taxanes.[33] Currently, the immunotherapy has modified the therapeutic scenario for these patients with the inclusion of pembrolizumab, atezolizumab and nivolumab as part of the first- and second-line therapy.[33] Interestingly, in second-line or further treatment, docetaxel is the approved treatment.[34] However, outcomes associated with conventional therapies remain poor, underlining the clear need for alternative approaches. The efficacy of the four more commonly used platinum-based chemotherapeutic regimens was evaluated in a randomized clinical trial in patients with advanced-stage NSCLC, resulting in survival rates of 33% at 1 year and 11% at 2 years.[11] Nevertheless, squamous lung carcinoma and ade- nocarcinomas do not always respond equally to chemotherapy and the combination with targeted therapies has extensively been tested with unsatisfactory results because of increased toxicity or lack of improvement in efficacy outcomes.[16,35,36] In 2008, a study comparing the efficacy of the combinations cis- platin plus gemcitabine *versus* cisplatin plus pemetrexed showed that squamous carcinomas were more sensitive to cis- platin plus gemcitabine while adenocarcinomas responded better to cisplatin plus pemetrexed.[14]

Here, we present *in vitro* and *in vivo* evidence showing that
treatment with ABTL0812 plus chemotherapy regimens com- monly used as first and second line in NSCLC patients, induced a dramatic synergistic reduction in cell viability and tumor growth in all cell line models tested, encompassing both adeno- carcinoma and squamous cell carcinoma. In all *in vivo* studies, ABTL0812 potentiated the anticancer effect of chemotherapy, significantly reducing tumor volume without increasing toxic- ity, including adenocarcinomas mutated in KRAS, where plati- num compounds remain as the primary treatment option, adenocarcinomas carrying an EGFR mutation (E790M) associ- ated with development of resistance to EGFR TKIs[31] and in squamous carcinomas wild-type or mutated in PTEN, where paclitaxel and carboplatin is often used as first-line. Impor- tantly, ABTL0812 potentiates chemotherapy without increasing toxicity in these murine models,

which correlate well with the good safety and tolerability profile that ABTL0812 showed in the first-in-humans trial carried out in metastatic and advanced solid tumors.[22] It also highlights ABTL0812 potential for clini- cal use overcoming the toxicity associated with the failure of different types of treatments.

Our study shows that the mechanism of cell death induced by the combined treatment of ABTL0812 and chemotherapy involves autophagy-mediated nonapoptotic cell death and provides an interesting link between synergy among these two pathways and loss of cell viability. In particular, combined treatment induced autophagic mediated nonapoptotic cell death that was dependent on TRIB3 upregulation. Accumulat- ing evidence reveals that autophagy and nonapoptotic cell death can cooperate, antagonize or assist each other, thus dif- ferentially influencing cell fate.[37,38] Interestingly, autophagy appears to facilitate nonapoptotic cell death in certain instances.[39,40] For example, in childhood acute lymphoblastic leukemia induction of autophagy-dependent necroptosis is required to overcome glucocorticoid resistance.[39] Further- more, Khan *et al*. has reported that palmitic acid triggers Ca^{2+}-dependent autophagy, resulting in the necroptosis of endo- thelial cells.[40] In our study, we have shown that chemotherapy treatment mainly induces apoptosis, meanwhile, the combina- tion of chemotherapy with ABTL0812 induces nonapoptotic cell death and autophagy. Interestingly, autophagy inhibition reverted the induction of cell death suggesting cell death induction by ABTL0812/chemotherapy combination is depen- dent on autophagy. This is in agreement with our previous results showing that ABTL0812 inhibits lung, pancreatic and endometrial cancer growth through autophagy induction.[20,21] Furthermore, other groups have reported that endoplasmic reticulum stress can promote autophagy and reduce chemo- therapy resistance in mutant p53 lung cancer cells.[41] More- over, other studies have shown that resistance to cisplatin in human lung cancer cells was mediated through autophagy impairment[42] and that autophagy induction re-sensitize cisplatin-resistant cells to cisplatin-induced cell death.[42] More- over, it has also been shown that induction of autophagy in nonsmall cell lung enhances pemetrexed cytotoxicity.[43] Hence, our results suggest that the induction of autophagy by ABTL0812 sensitize lung cancer cells to chemotherapy finally leading to nonapoptotic cell death.

Our in vitro and in vivo data provided evidence that TRIB3 is one of the important genes involved in mediating ABTL0812/chemotherapy induced cell death, and that TRIB3/ autophagy signaling participated in this process. The “pseudokinase” function of TRIB3 facilitates the inactivation of multiple transcription factors and signaling proteins.44 TRIB3 is expressed in a variety of human cells where it plays different roles in cell apoptosis, autophagy and migration among other cellular functions.45,46 The role of TRIB3 in human cancer remains controversial, presumable because it largely depends on the biological context, where depending on the cell type and the stimuli it can either inhibit or promote tumor growth.47–49 For example, TRIB3 has been found to be overexpressed in lung cancer tissues in patients with NSCLC47 and its inhibition in A549 lung adenocarcinoma cells induced apoptosis.47 On the contrary, it has been shown that TRIB3 has oncosuppressive functions and that TRIB3 loss promotes Akt-driven tumorigenesis in vitro and in vivo,25,30 correlating with our previous reports showing how ABTL0812 inhibits the Akt/mTORC1 axis and induces autophagy-mediated can- cer cell death by upregulating TRIB3 in lung and pancreatic cancer models.21 ABTL0812-mediated TRIB3 upregulation is potentiated when combined with chemotherapy, sensitizing lung cancer cells to chemotherapy and inhibiting tumor growth in vitro and in vivo. In agreement with our data, Sala- zar et al. have shown that TRIB3 reverses Akt-mediated che-motherapy resistance in human hepatocellular carcinoma cells.50

ABTL0812 is currently under Phase II clinical development for patients with squamous NSCLC and endometrial carci- noma as first-line in combination with SOC carboplatin/pacli- taxel (NCT03366480). Our preliminary clinical results showed that in patients treated with ABTL0812, TRIB3 is upregulated in whole blood 1 week after the first dose and that this upregulation is maintained 3 weeks after the first chemother- apy dose. TRIB3 upregulation varies among patients showing high variability and although there is a clear trend, further studies relating TRIB3 expression with efficacy must be done in order to potentially associate it with response rates. Although further research is needed, these results

suggest that TRIB3 can be used as a pharmacodynamic biomarker to fol- low ABTL0812 activity in human patients.

Together with these studies, our results suggest that thera- peutic strategies that activate TRIB3, such as treatment with ABTL0812, could be an attractive new therapeutic option to inhibit tumor growth, potentiate chemotherapy effect and overcome resistance. These findings improve the understand- ing of the mechanisms of the anticancer activity of ABTL0812 against lung cancer and provide a theoretical basis for the clinical application of novel ABTL0812/chemotherapy-based combinations in the future.

Acknowledgements

This work was performed at IDIBAPS (CERCA Programme/Generalitat de Catalunya), UB (Barcelona University) and UAB (Autonomous Uni- versity of Barcelona). This work was supported by grants from Cellex Foundation, Froi Foundation, Instituto de Salud Carlos III through the projects PI15/00661 and RTICC and RETOS RD12/00360055 and RD12/0036/0070 (Co-funded by European Regional Development Fund) -Investing in your future-" Spanish Ministry of Economy and Competitiveness (MINECO), (EMPLEA/EMP-TU-2015-4576 and Centre for the Development of Industrial Technology (CDTI, INNOGLOBAL/20171061), Secretaria d'Universitats i Recerca del Departament d'Economia i Con- eixement (2014_SGR_530, 2017_SGR_1305 and 2014_SGR_740) and BBVA (becas Leonardo 2018, BBM-TRA-0041). P.B. had a Beatriu Pinos postdoctoral fellowship "AGAUR; BP-B 00160" (Co-funded by European Union). P.F-N. and A.N-C. have been funded by APIF fellowships from the University of Barcelona, School of Medicine, L.R-P has a FPU predoc- toral fellowship.

Conflict of interest

ABTL0812 is a drug under development by Ability Pharmaceuti- cals. P.M-G., S.S-S., E.M-R., H.P-M., M.Y-V., C.D. and J.A. are
Ability Pharmaceuticals employees; C.D. is a founder of Ability Pharmaceuticals and holds shares of the company; E.N. has received consultancy fees from Ability Pharmaceuticals;
J.M.L. and P.G. are members of its Scientific Advisory Board

REFERENCES

1. Ridge CA, McErlean AM, Ginsberg MS. Epidemi- ology of lung cancer. *Semin Intervent Radiol* 2013; 30:93–8.
2. Siegel R, Ma J, Zou Z, et al. Cancer statistics, 2014. *CA Cancer J Clin* 2014;64:9–29.
3. Siegel RL, Miller KD, Jemal A. Cancer statistics, 2017. *CA Cancer J Clin* 2017;67:7–30.
4. Couraud S, Zalcman G, Milleron B, et al. Lung cancer in never smokers—a review. *Eur J Cancer* 2012;48:1299–311.
5. Zappa C, Mousa SA. Non-small cell lung cancer: current treatment and future advances. *Transl Lung Cancer Res* 2016;5:288–300.
6. Howington JA, Blum MG, Chang AC, et al. Treat- ment of stage I and II non-small cell lung cancer: diagnosis and management of lung cancer, 3rd ed: American College of Chest Physicians evidence-based clinical practice guidelines. *Chest* 2013;143: e278S–313S.
7. Delbaldo C, Michiels S, Syz N, et al. Benefits of adding a drug to a single-agent or a 2-agent che- motherapy regimen in advanced non-small-cell lung cancer: a meta-analysis. *JAMA* 2004;292: 470–84.
8. Goffin J, Lacchetti C, Ellis PM, et al. Lung cancer disease site Group of Cancer Care Ontario's pro- gram in evidence-based C. first-line systemic che- motherapy in the treatment of advanced non-small cell lung cancer: a systematic review. *J Thorac Oncol* 2010;5:260–74.
9. Reck M, Rodriguez-Abreu D, Robinson AG, et al. Pembrolizumab versus chemotherapy for PD-L1-positive non-small-cell lung cancer. *N Engl J Med* 2016;375:1823–33.

10. Hellmann MD, Paz-Ares L, Bernabe Caro R, et al. Nivolumab plus Ipilimumab in advanced non-small-cell lung cancer. *N EnglJ Med* 2019;381:2020–31.
11. Schiller JH, Harrington D, Belani CP, et al. Com- parison of four chemotherapy regimens for advanced non-small-cell lung cancer. *N Engl J Med* 2002;346:92–8.
12. Belani CP, Ramalingam S, Perry MC, et al. Ran- domized, phase III study of weekly paclitaxel in combination with carboplatin versus standard every-3-weeks administration of carboplatin and paclitaxel for patients with previously untreated advanced non-small-cell lung cancer. *J Clin Oncol* 2008;26:468–73.
13. Ramalingam S, Perry MC, La Rocca RV, et al. Comparison of outcomes for elderly patients treated with weekly paclitaxel in combination with carboplatin versus the standard 3-weekly pacli- taxel and carboplatin for advanced nonsmall cell lung cancer. *Cancer* 2008;113:542–6.
14. Scagliotti GV, Parikh P, von Pawel J, et al. Phase III study comparing cisplatin plus gemcitabine with cisplatin plus pemetrexed in chemotherapy- naive patients with advanced-stage non-small-cell lung cancer. *J Clin Oncol* 2008;26:3543–51.
15. Zinner RG, Fossella FV, Gladish GW, et al. Phase II study of pemetrexed in combination with car- boplatin in the first-line treatment of advanced nonsmall cell lung cancer. *Cancer* 2005;104: 2449–56.

Socinski MA, Bondarenko I, Karaseva NA, et al. Weekly nab-paclitaxel in combination with car- boplatin versus solvent-based paclitaxel plus car- boplatin as first-line therapy in patients with advanced non-small-cell lung cancer: final results of a phase III trial. *J Clin Oncol* 2012;30:2055–62.
Falasca M, Selvaggi F, Buus R, et al. Targeting phosphoinositide 3-kinase pathways in pancreatic cancer—from molecular signalling to clinical tri- als. *Anticancer Agents Med Chem* 2011;11:455–63.
16. West KA, Castillo SS, Dennis PA. Activation of the PI3K/Akt pathway and chemotherapeutic resistance. *Drug Resist Updat* 2002;5:234–48.
17. Guertin DA, Sabatini DM. Defining the role of mTOR in cancer. *Cancer Cell* 2007;12:9–22.
18. Felip I, Moiola CP, Megino-Luque C, et al. Thera- peutic potential of the new TRIB3-mediated cell autophagy anticancer drug ABTL0812 in endome- trial cancer. *Gynecol Oncol* 2019;153:425–35.
19. Erazo T, Lorente M, Lopez-Plana A, et al. The new antitumor drug ABTL0812 inhibits the Akt/- mTORC1 Axis by upregulating tribbles-3 pseudokinase. *Clin Cancer Res* 2016;22:2508–19.
20. Boixader LV, Gaba L, Victoria I, et al. Dose- escalation of the first-in human phase I/Ib study of ABTL0812, a novel antitumor drug inhibiting the Akt/mTOR pathway in patients with advanced solid tumors. *J Clin Oncol* 2015;33:2585.
21. Mathur A, Abd Elmageed ZY, Liu X, et al. Sub- verting ER-stress towards apoptosis by nelfinavir and curcumin coexposure augments docetaxel efficacy in castration resistant prostate cancer cells. *PLoS One* 2014;9:e103109.
22. Ravanan P, Srikumar IF, Talwar P. Autophagy: the spotlight for cellular stress responses. *Life Sci* 2017;188:53–67.
23. Garcia D, Shaw RJ. AMPK: mechanisms of cellu- lar energy sensing and restoration of metabolic balance. *Mol Cell* 2017;66:789–800.
24. Faubert B, Vincent EE, Griss T, et al. Loss of the tumor suppressor LKB1 promotes metabolic reprogramming of cancer cells via HIF-1alpha. *Proc Natl Acad Sci USA* 2014;111:2554–9.
25. Chou T-C. Theoretical basis, experimental design, and computerized simulation of synergism and antagonism in drug combination studies. *Pharmacol Rev* 2006;58:621–81.
26. Chou T-C. Drug combination studies and their synergy quantification using the Chou-Talalay method. *Cancer Res* 2010;70:440–6.
27. Sun Z, Wang Z, Liu X, et al. New development of inhibitors targeting the PI3K/AKT/Mtor pathway in personalized treatment of non-small- cell lung cancer. *Anticancer Drugs* 2015;26:1–14.
28. Mauthe M, Orhon I, Rocchi C, et al. Chloroquine inhibits autophagic flux by decreasing autophagosome-lysosome fusion. *Autophagy* 2018; 14:1435–55.
29. Ma F, Xu B, Lin D, et al. Effect of rs2293347 poly- morphism in EGFR on the clinical efficacy of Gefitinib in patients with non-small cell lung can- cer. *Zhongguo Fei Ai Za Zhi* 2011;14:642–5.
30. Thomas A, Liu SV, Subramaniam DS, et al. Refin- ing the treatment of NSCLC according to histo- logical

and molecular subtypes. *Nat Rev Clin Oncol* 2015;12:511–26.
31. Ettinger DS, Aisner DL, Wood DE, et al. NCCN guidelines insights: non-small cell lung cancer, ver- sion 5.2018. *J Natl Compr Canc Netw* 2018;16: 807–21.
32. Peters S, Adjei AA, Gridelli C, et al. Metastatic non-small-cell lung cancer (NSCLC): ESMO clini- cal practice guidelines for diagnosis, treatment and follow-up. *Ann Oncol* 2012;23(Suppl 7):vii56–64.
33. Socinski MA, Stinchcombe TE, Moore DT, et al. Incorporating bevacizumab and erlotinib in the combined-modality treatment of stage III non- small-cell lung cancer: results of a phase I/II trial. *J Clin Oncol* 2012;30:3953–9.
34. Ramalingam SS, Maitland ML, Frankel P, et al. Carboplatin and paclitaxel in combination with either vorinostat or placebo for first-line therapy of advanced non-small-cell lung cancer. *J Clin Oncol* 2010;28:56–62.
35. Bareford MD, Park MA, Yacoub A, et al. Sorafenib enhances pemetrexed cytotoxicity through an autophagy-dependent mechanism in cancer cells. *Cancer Res* 2011;71:4955–67.
36. Nikoletopoulou V, Markaki M, Palikaras K, et al. Crosstalk between apoptosis, necrosis and autophagy. *Biochim Biophys Acta* 2013;1833:3448–59.
37. Bonapace L, Bornhauser BC, Schmitz M, et al. Induction of autophagy-dependent necroptosis is required for childhood acute lymphoblastic leuke- mia cells to overcome glucocorticoid resistance *J Clin Invest* 2010;120:1310–23.
38. Khan MJ, Rizwan Alam M, Waldeck- Weiermair M, et al. Inhibition of autophagy res- cues palmitic acid-induced necroptosis of endo- thelial cells. *J Biol Chem* 2012;287:21110–20.
39. Gan PP, Zhou YY, Zhong MZ, et al. Endoplasmic reticulum stress promotes autophagy and apopto- sis and reduces chemotherapy resistance in mutant p53 lung cancer cells. *Cell Physiol Biochem* 2017;44:133–51.
40. Sirichanchuen B, Pengsuparp T, Chanvorachote P. Long-term cisplatin exposure impairs autophagy and causes cisplatin resistance in human lung can- cer cells. *Mol Cell Biochem* 2012;364:11–8.
41. del Bufalo D, Desideri M, de Luca T, et al. His- tone deacetylase inhibition synergistically enhances pemetrexed cytotoxicity through induc- tion of apoptosis and autophagy in non-small cell lung cancer. *Mol Cancer* 2014;13:230.
42. Eyers PA, Keeshan K, Kannan N. Tribbles in the 21st century: the evolving roles of tribbles pseudokinases in biology and disease. *Trends Cell Biol* 2017;27:284–98.
43. Mondal D, Mathur A, Chandra PK. Tripping on TRIB3 at the junction of health, metabolic dys- function and cancer. *Biochimie* 2016;124:34–52.
44. Salazar M, Lorente M, Orea-Soufi A, et al. Oncosuppressive functions of tribbles pseudokinase 3. *Biochem Soc Trans* 2015;43:1122–6.
45. Zhou H, Luo Y, Chen JH, et al. Knockdown of TRB3 induces apoptosis in human lung adenocar- cinoma cells through regulation of notch 1 expres- sion. *Mol Med Rep* 2013;8:47–52.
46. Ding CZ, Guo XF, Wang GL, et al. High glucose contributes to the proliferation and migration of non-small cell lung cancer cells via GAS5-TRIB3 axis. *Biosci Rep* 2018;38:BSR20171014.
47. Su J, Yan Y, Qu J, et al. Emodin induces apoptosis of lung cancer cells through ER stress and the TRIB3/NF-kappaB pathway. *Oncol Rep* 2018;37:1565–72.
48. Li Y, Zhu D, Hou L, et al. TRB3 reverses chemo- therapy resistance and mediates crosstalk between endoplasmic reticulum stress and AKT signaling pathways in MHCC97H human hepatocellular carcinoma cells. *Oncol Lett* 2018;15:1343–9.

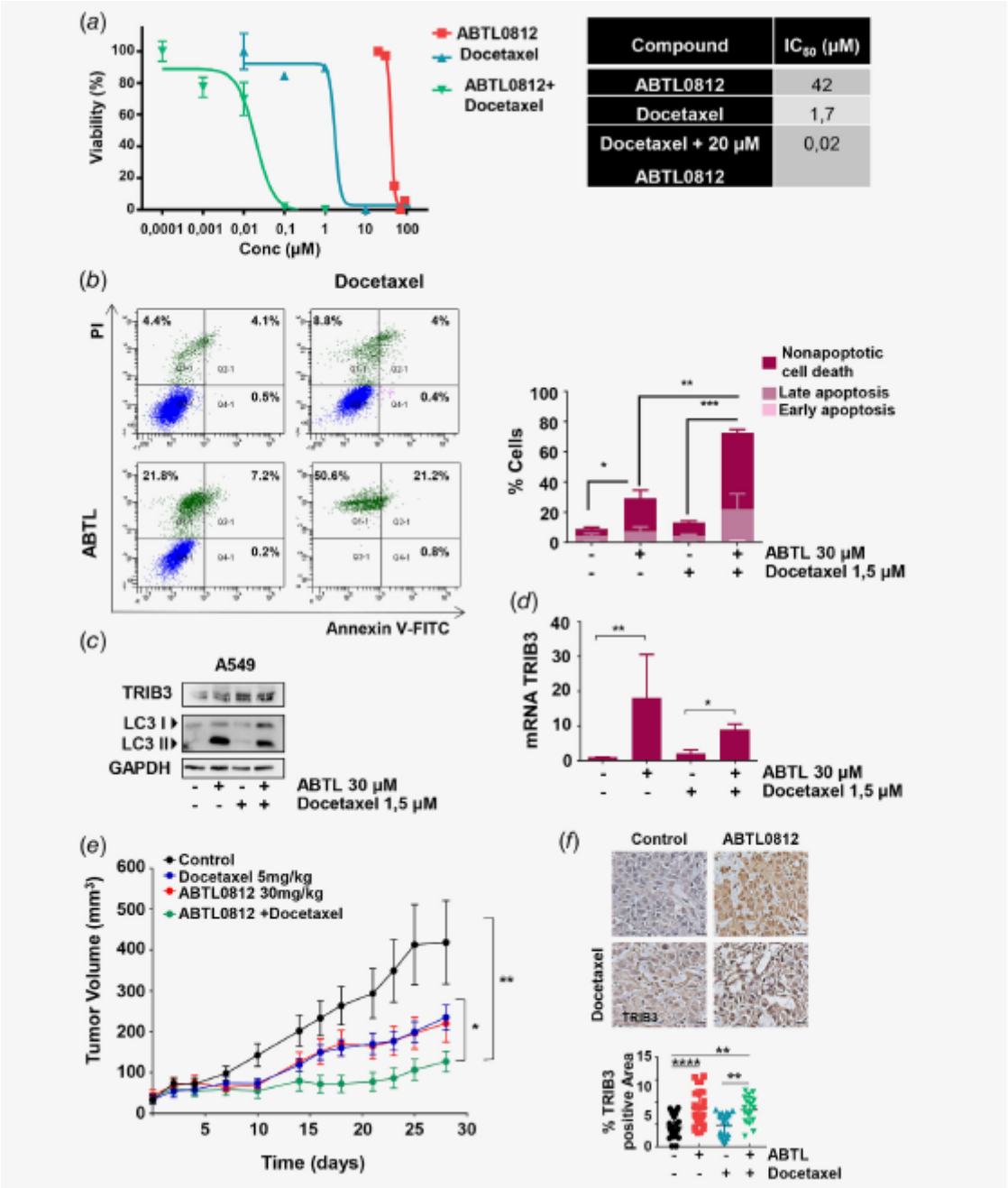

Figure 1. ABTL0812 potentiates docetaxel antitumor activity in lung adenocarcinomas by inducing TRIB3 activation and autophagy. (*a*) Adenocarcinoma A549 lung cancer cell lines viability after treatment for 72 hr with increasing concentrations of ABTL0812 (0–200 µM), docetaxel (0–100 µM) or suboptimal concentrations of ABTL0812 (20 µM) combined with increasing concentrations of docetaxel (0–100 µM). The graphs show the percentage of viability. Data represent mean ± SD, *n* = 3. Table showing IC_{50} (95% confidence interval for each treatment) for adenocarcinoma A549 treatments from curves in A. (*b*) Flow cytometry diagram (left panel) and quantification (right graph) of the percentage of annexin-V/PI-positive cells in adenocarcinoma A549 lung cancer cells treated with ABTL0812 (30 µM) or docetaxel (1.5 µM) alone or in combination for 48 hr. The numbers represent the percentage of events. Data represent mean ± SD, *n* = 3. **p* < 0.05, ***p* < 0.01 and ****p* < 0.001 by ANOVA with Sidak *post hoc* multiple comparison test. (*c*) Western blot showing TRIB3 and LC3 total levels in adenocarcinoma A549 lung cancer cell lines treated with ABTL0812 (30 µM) or docetaxel (1.5 µM) alone or in combination for 48 hr. (*d*) *TRIB3* qPCR in adenocarcinoma A549 lung cancer cell lines treated with ABTL0812 (30 µM) or docetaxel (1.5 µM) alone or in combination for 48 hr. Data represent mean ± SD, *n* = 3. **p* < 0.05 and ***p* < 0.01 by ANOVA with Sidak *post hoc* multiple comparison test. (*e*) Tumor growth of subcutaneously implanted adenocarcinoma A549 lung cancer cells

treated with vehicle (*n* = 8), ABTL0812 (*n* = 8; 30 mg/kg), docetaxel
(*n* = 8; 5 mg/kg) or a combination of ABTL0812 and docetaxel (*n* = 8) for 28 days. The data are expressed as an increase in tumor volume using treatment Day 0 as a reference. Data represent mean ± SD, **p* < 0.05 and ***p* < 0.01 by ANOVA with Sidak *post hoc* multiple comparison test. (*f*) Representative images showing TRIB3 staining in the adenocarcinoma A549 lung cancer cells derived tumors treated with ABTL0812 (30 mg/kg), docetaxel (5 mg/kg) or a combination of ABTL0812 and docetaxel for 28 days. Scale bar 100 µm.

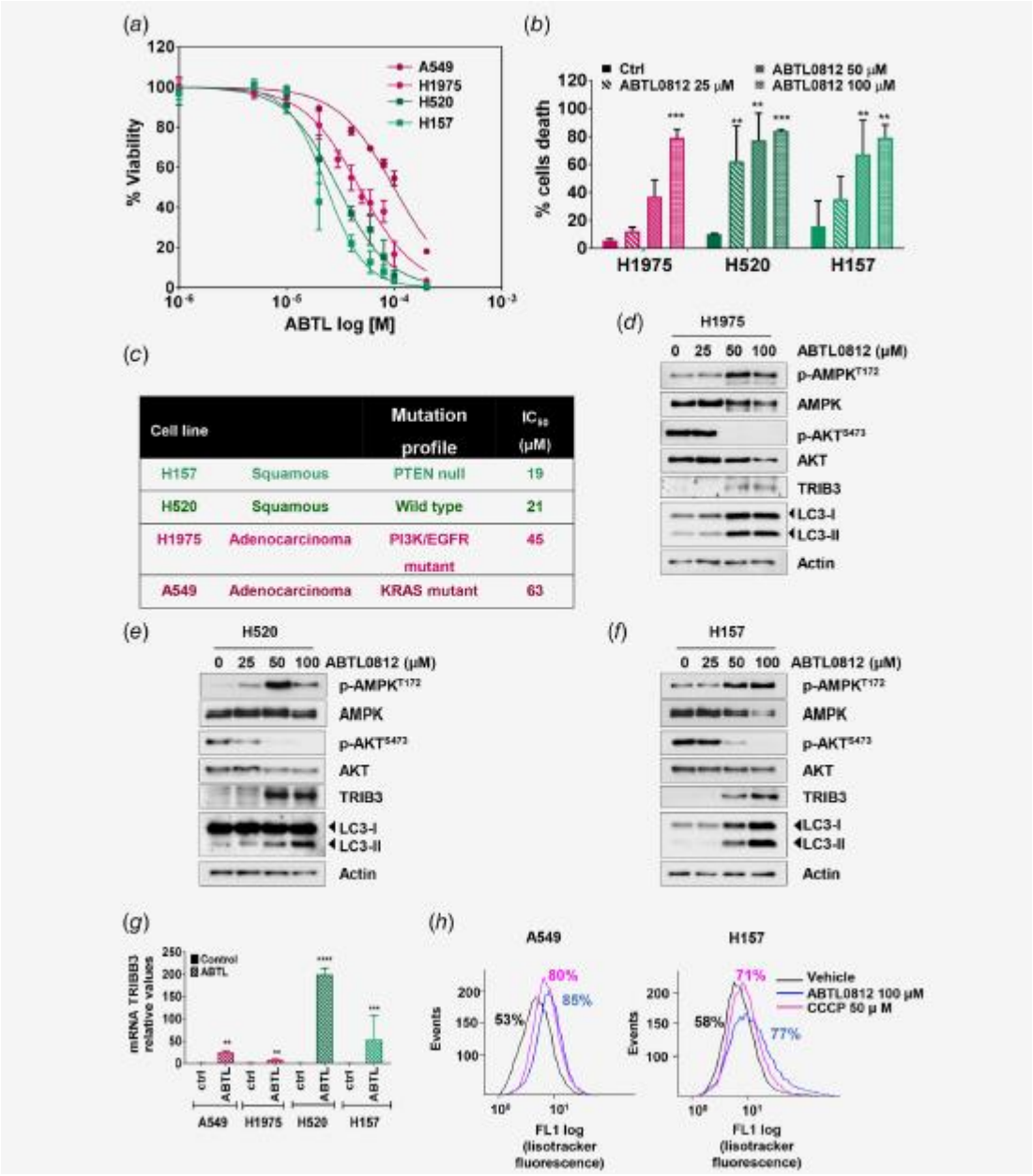

Figure 2. ABTL0812 induces cell death and inhibits AKT/mTOR axis in both squamous and lung adenocarcinomas through *TRIB3* upregulation, autophagy and AKT inhibition. (*a*) Cell viability was quantified in adenocarcinoma (A549 and H1975) and squamous (H157 and H520) lung cancer cell lines treated for 48 hr with increasing doses of ABTL0812 (0–200 µM). Squamous cells were represented with green lines and adenocarcinoma cells are represented with pink lines. Graphs show the percentage of cell viability for each dose. Data represent mean ± SD, $n = 3$. (*b*) Graphs show percentage of adenocarcinoma (A549 and H1975) and squamous (H157 and H520) lung cancer cell lines cell death under ABTL0812 treatments (25–100 µM) for 24 hr measured with Trypan blue. Data represent mean ± SD, $n = 3$. Significant differences by ANOVA with Sidak *post hoc* multiple comparison test are indicated as $^{**}p < 0.01$ and $^{***}p < 0.001$. (*c*) Table showing tumor type origin, mutation profile and IC_{50} (95% confidence interval for each treatment) for adenocarcinoma (A549 and H1975) and squamous (H157 and H520) lung cancer cell lines treatments with ABTL0812 from curves in *a*. (*d*) Western blot showing phospho-AMPK (T172), total AMPK, phospho-AKT (ser473), total AKT, LC3 processing and TRIB3 total levels in adenocarcinoma lung cancer H1975 cells treated with increasing doses of ABTL0812 (25, 50 and 100 µM) for 24 hr. Data represent mean ± SD, $n = 3$. (*e*) Western blot showing phospho-AMPK (T172), total AMPK, phospho-AKT (ser473), total AKT, LC3 processing and TRIB3 total levels in squamous H520 lung cancer cells treated with increasing doses of ABTL0812 (25, 50 and 100 µM) for 24 hr. Data represent mean ± SD, $n = 3$. (*f*) Western blot showing phospho-AMPK (T172),

total AMPK, phospho-AKT (ser473), total AKT, LC3 processing and TRIB3 total levels in squamous H157 lung cancer cells treated with increasing doses of ABTL0812 (25, 50 and 100 µM) for 24 hr. Data represent mean ± SD, $n = 3$. (*g*) *TRIB*3 qPCR in a panel of adenocarcinoma (H1975 and A549) and squamous (H157 and H520) lung cancer cell lines treated with ABTL0812 (15 µM) for 24 hr. Data represent mean ± SD, $n = 3$.
$^{*}p < 0.05$ and $^{**}p < 0.01$ by ANOVA with Sidak *post hoc* multiple comparison test. (*h*) Representative histograms. Flow cytometry analysis of intracellular ROS using the DFCH-DA probe. A549 and H157 cells were treated for 6 hr with ABTL0812 100 µM (blue line), CCCP 50 µM (positive control; pink line) or maintained untreated (control; Black line). The numbers represent the percentage of events.

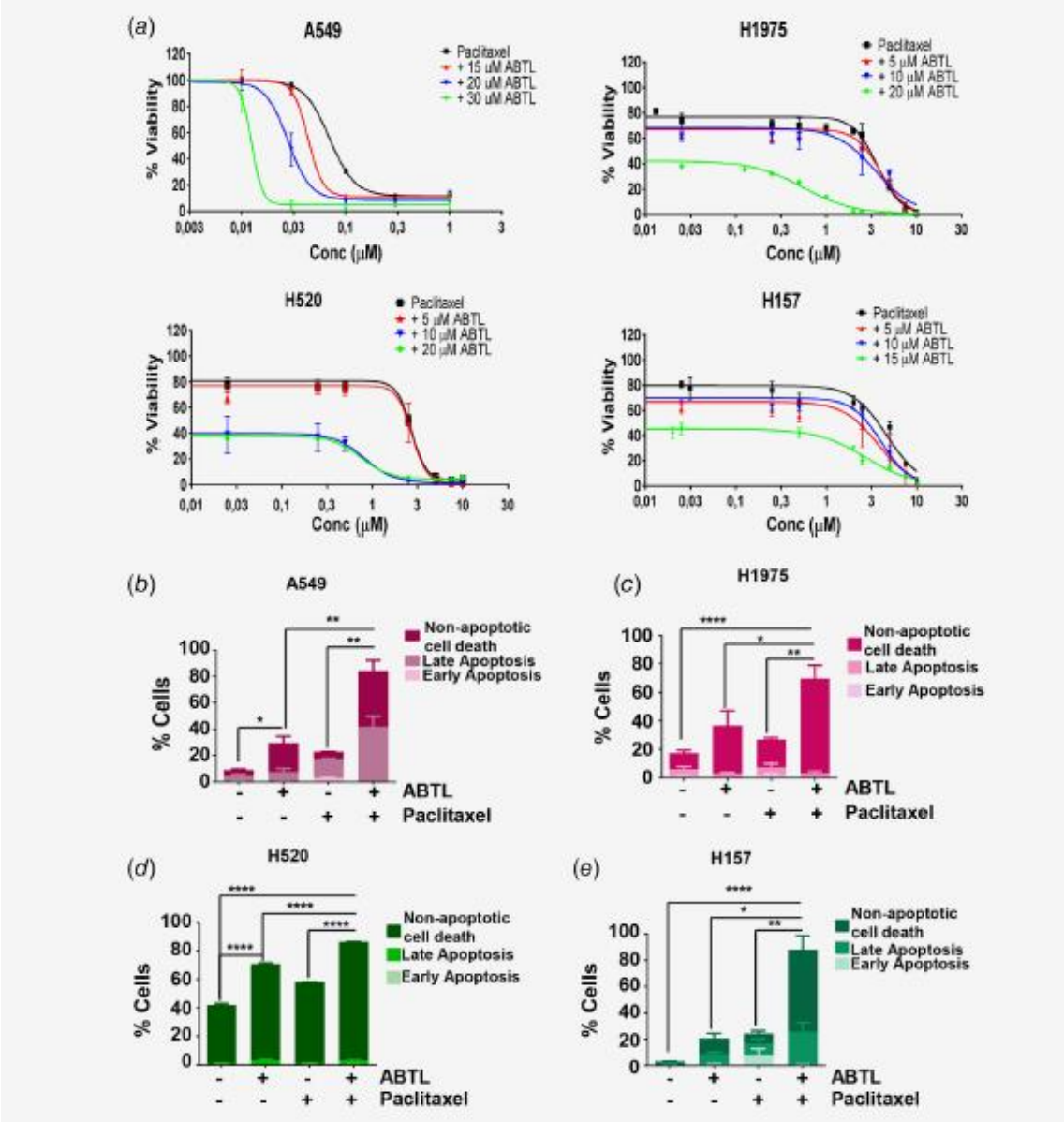

Figure 3. ABTL0812 synergistically potentiates the cytotoxicity of paclitaxel in adenocarcinoma and squamous lung cancer cells. (*a*) Upper left panel: adenocarcinoma A549 lung cancer cells viability after treatment for 72 hr with increasing concentrations of paclitaxel (0–1 μM), or
sub-IC50 concentrations of ABTL0812 (15, 20 or 30 μM) combined with increasing concentrations of paclitaxel (0–1 μM). Upper right graph: Adenocarcinoma H1975 lung cancer cells viability after treatment for 48 hr with increasing concentrations of paclitaxel (0–1 μM), or sub-IC50 concentrations of ABTL0812 (5, 10 or 20 μM) combined with increasing concentrations of paclitaxel (0–1 μM). Lower left panel: squamous H520 lung cancer cells viability after treatment for 48 hr with increasing concentrations of paclitaxel (0–1 μM), or sub-IC50 concentrations of ABTL0812 (5, 10 or 20 μM) combined with increasing concentrations of paclitaxel (0–1 μM). Lower right panel: squamous H157 lung cancer cells viability after treatment for 48 hr with increasing concentrations of paclitaxel (0–1 μM), or sub-IC50 concentrations of ABTL0812
(5, 10 or 15 μM) combined with increasing concentrations of paclitaxel (0–1 μM). The graphs show the percentage of viability. Data represent mean ± SD, $n = 3$. (*b*) Quantification of the percentage of annexin-V/PI-positive cells in adenocarcinoma A549 lung cancer cells treated with ABTL0812 (30 μM) or paclitaxel (1 μM) alone or in combination for 48 hr. Data represent mean ± SD, $n = 3$. *$p < 0.05$ and **$p < 0.01$ by ANOVA with Sidak *post hoc* multiple comparison test. (*c*) Quantification of the percentage of annexin-V/PI-positive cells in adenocarcinoma H1975 lung cancer cells treated with ABTL0812 (30 μM) or paclitaxel (0.75 μM) alone or in combination for 48 hr. Data represent mean ± SD, $n = 3$. *$p < 0.05$, **$p < 0.01$, ***$p < 0.001$ and ****$p < 0.0001$ by ANOVA with Sidak *post hoc* multiple comparison test. (*d*) Quantification of the percentage of annexin-V/PI-positive cells in

squamous H520 lung cancer cells treated with ABTL0812 (10 µM) or paclitaxel (0.2 µM) alone or in combination for 48 hr. Data represent mean ± SD, $n = 3$. *$p < 0.05$, **$p < 0.01$, ***$p < 0.001$ and ****$p < 0.0001$ by ANOVA with Sidak *post hoc* multiple comparison test. (*e*) Quantification of the percentage of annexin-V/PI-positive cells in squamous H157 lung cancer cells treated with ABTL0812 (10 µM) or paclitaxel (0.5 µM) alone or in combination for 48 hr. Data represent mean ± SD, $n = 3$. *$p < 0.05$,
**$p < 0.01$, ***$p < 0.001$ and ****$p < 0.0001$ by ANOVA with Sidak *post hoc* multiple comparison test.

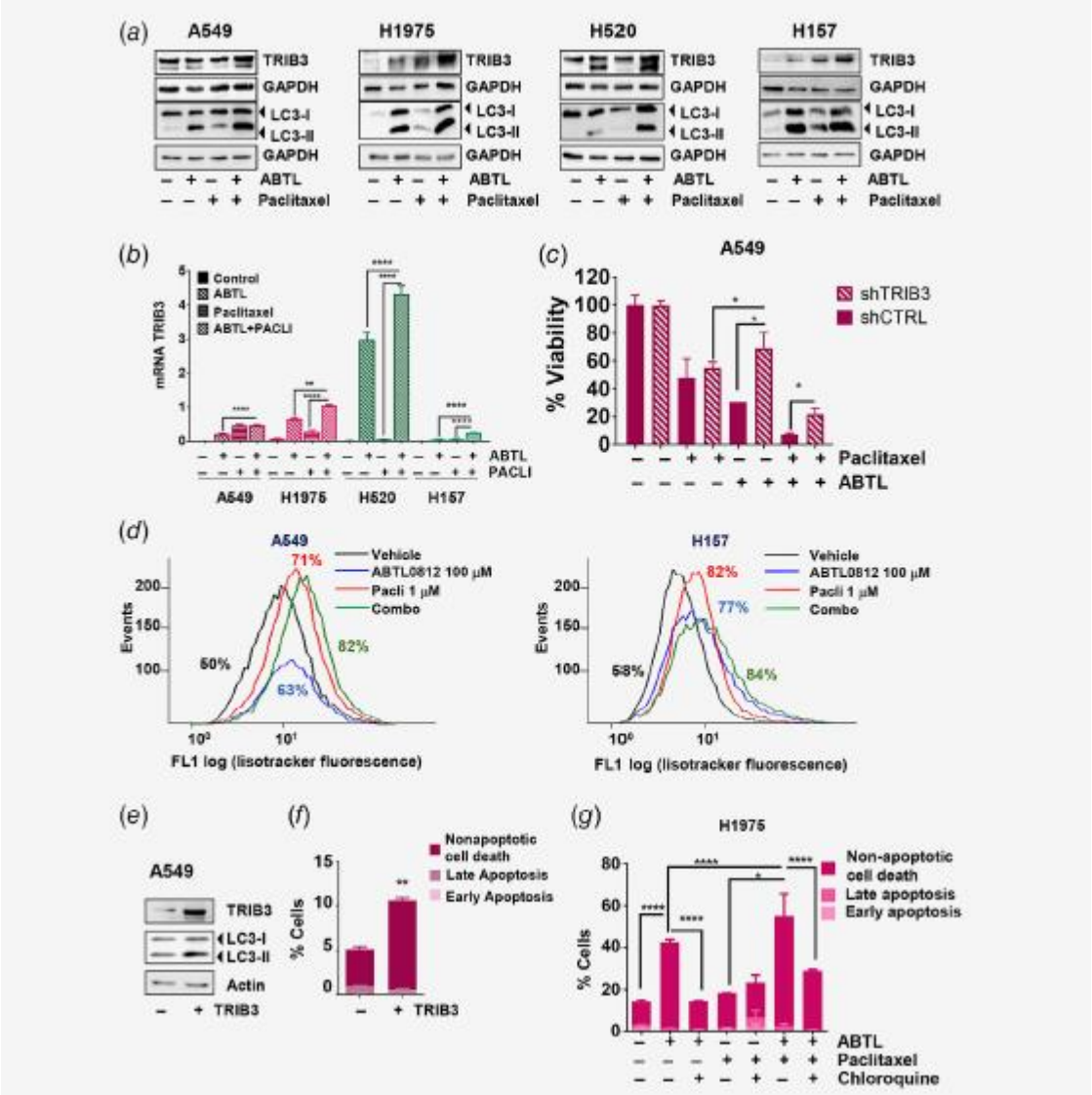

Figure 4. ABTL0812 potentiates chemotherapy effect through autophagy promotion and TRIB3 induction of nonapoptotic cell death. (*a*) Western blot showing LC3 processing, and TRIB3 total levels in adenocarcinoma A549 lung cancer cells treated with ABTL0812 (30 µM) and paclitaxel (3 µM) alone or in combination for 24 hr, in adenocarcinoma H1975 lung cancer cells treated with ABTL0812 (30 µM) and paclitaxel (0.75 µM) alone or in combination for 24 hr, in squamous H520 lung cancer cells treated with ABTL0812 (10 µM) and paclitaxel (0.2 µM) alone or in combination for 24 hr and in squamous H157 lung cancer cells treated with ABTL0812 (15 µM) and paclitaxel (0.75 µM) alone or in combination for 24 hr. (*b*) *TRIB*3 qPCR in a panel of adenocarcinoma (H1975 and A549) and squamous (H157 and H520) lung cancer cell lines treated with ABTL0812 and paclitaxel alone or in combination (cell line dependent, same conditions as in western blot in *a*) for 24 hr. Data represent mean ± SD, $n = 3$. *$p < 0.05$, **$p < 0.01$, ***$p < 0.001$ and ****$p < 0.0001$ by ANOVA with Sidak *post hoc* multiple comparison test. (*c*) A549 control and shTRIB3 clone's viability after treatment for 48 hr with paclitaxel (1 µM), ABTL0812 (30 µM) or a combination of both. (*d*) Representative Histograms. Flow cytometry analysis of intracellular ROS using the DFCH-DA probe. A549 and H157 cells were treated for 6 hr with ABTL0812 100 µM (blue line), paclitaxel 1 µM (red line), a combination of both (green) or maintained untreated (control; Black line). The numbers represent the percentage of events in each treatment. (*e*) TRIB3 and LC3 western blot in A549 cells transfected with a control vector or a TRIB3 vector for 24 hr. (*f*) Quantification of the percentage of annexin-V/PI-positive cells in A549 lung cancer cells transfected with a control vector or a TRIB3 vector for 48 hr. *$p < 0.05$. (*g*) Percentage of annexin-V/PI-positive cells in adenocarcinoma H1975 lung cancer cells pretreated with the autophagy inhibitor chloroquine (20 µM) for 3 hr. Cells were then treated with ABTL0812(30 µM), paclitaxel (0.75 µM) alone or in combination in the presence or absence of chloroquine for 48 hr. Data represent mean ± SD, $n = 3$. *$p < 0.05$, **$p < 0.01$, ***$p < 0.001$ and ****$p < 0.0001$ by ANOVA with Sidak *post hoc* multiple comparison test.

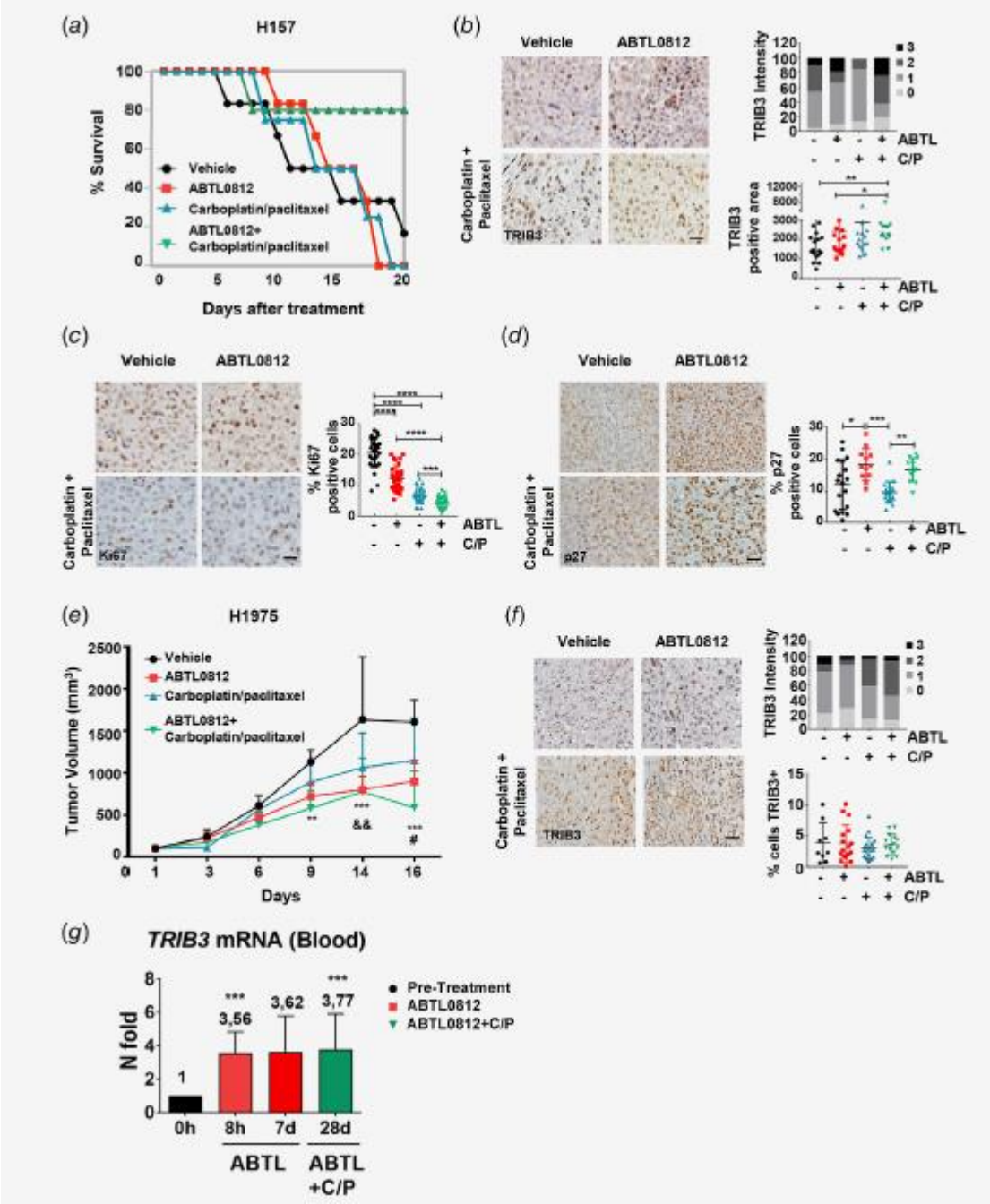

Figure 5. ABTL0812 enhanced carboplatin and paclitaxel antitumor activity both in adenocarcinomas and squamous lung xenografts. (*a*) Percentage of survival in nude mice subcutaneously implanted with squamous H157 cells and treated with vehicle (*n* = 8), ABTL0812 (*n* = 8; 120 mg/kg), carboplatin/paclitaxel (*n* = 8; 20/5 mg/kg) or a combination of ABTL0812 with carboplatin/paclitaxel (*n* = 8) for 20 days. The data are expressed as days. (*b*) Representative images showing TRIB3 staining in squamous H157 lung cancer cells derived tumors treated with ABTL0812 (120 mg/kg), carboplatin/paclitaxel (20/5 mg/kg) or a combination of ABTL0812 with carboplatin/paclitaxel for 20 days.

Scale bar 100 µm. Graphs represent TRIB3 quantification as intensity (upper graph) and positive area (lower graph). (*c*) Representative images showing KI67 staining in the squamous H157 lung cancer cells derived tumors treated with ABTL0812 (120 mg/kg), carboplatin/ paclitaxel (20/5 mg/kg) or a combination of ABTL0812 with carboplatin/paclitaxel for 20 days. Scale bar 100 µm. Graph represents KI67 quantification as percentage of KI67 positive cells. (*d*) Representative images showing p27 staining in the squamous H157 lung cancer cells derived tumors treated with ABTL0812 (120 mg/kg), carboplatin/paclitaxel (20/5 mg/kg) or a combination of ABTL0812 with carboplatin/ paclitaxel for 20 days. Scale bar 100 µm. Graph represents p27 quantification as percentage of

p27 positive cells. (*e*) Tumor growth of subcutaneously implanted adenocarcinoma H1975 lung cancer cells in nude mice treated with vehicle (n = 7), ABTL0812 (n = 9; 120 mg/kg), carboplatin/paclitaxel (n = 9; 10/5 mg/kg) or a combination of ABTL0812 with carboplatin/paclitaxel (n = 9) for 20 days. The data are expressed as tumor volume increment using treatment Day 0 volumes as a reference. Data represent mean ± SD, n = 5. **p < 0.01, ***p < 0.001, &&, #, by ANOVA with Sidak *post hoc* multiple comparison test. (*f*) Representative images showing TRIB3 staining in the adenocarcinoma H1975 lung cancer cells derived tumors treated with ABTL0812 (120 mg/kg), carboplatin/paclitaxel (10/5 mg/kg) or a combination of ABTL0812 with carboplatin/paclitaxel for 21 days. Scale bar 100 µm. Graphs represent TRIB3 quantification as intensity (upper graph) and positive area (lower graph). (*g*) *TRIB*3 qPCR in PBMCs from blood samples from patients under chronic treatment with ABTL0812 (1,300 mg tid: basal level). Samples were collected: 8 hr after the first dose of ABTL0812, 1 week after the first dose of ABTL0812 and 28 days after the first dose of ABTL0812 (and 3 weeks after having received the first cycle of chemotherapy in combination with ABTL0812).

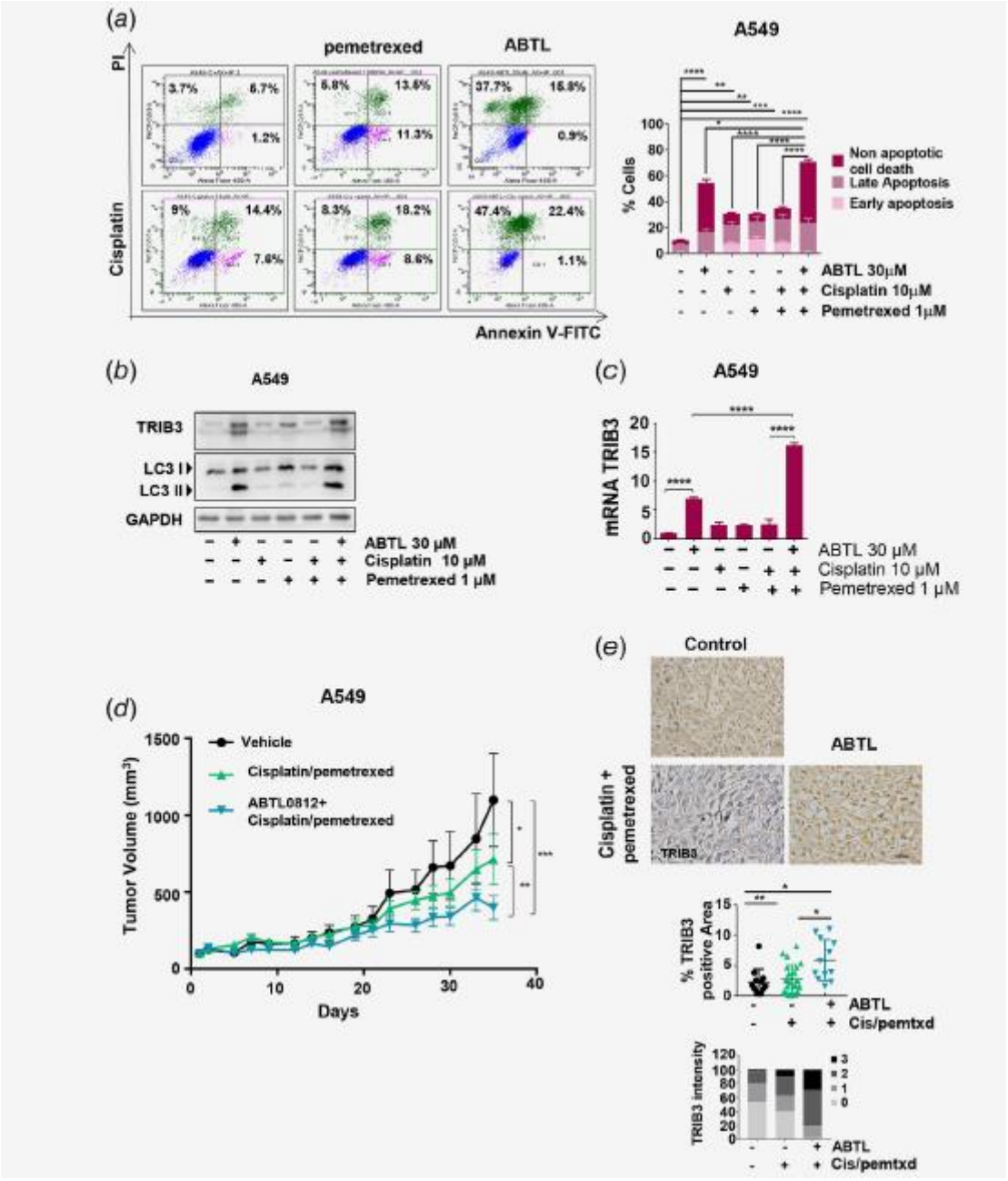

Figure 6. ABTL0812 potentiated cisplatin and pemetrexed antitumor activity *in vivo*. (*a*) Flow cytometry diagram (left panel) and quantification (right graph) of the percentage of annexin-V/PI-positive cells in adenocarcinoma A549 lung cancer cells treated with ABTL0812 (30 μM), cisplatin (10 μM), pemetrexed (1 μM) alone or in combination for 48 hr. The numbers represent the percentage of events. Data represent mean ± SD, $n = 3$. *$p < 0.05$, **$p < 0.01$, ***$p < 0.001$ and ****$p < 0.0001$ by ANOVA with Sidak *post hoc* multiple comparison test. (*b*) Western blot showing LC3 processing, and TRIB3 total levels in adenocarcinoma A549 lung cancer cells treated with ABTL0812 (30 μM), cisplatin (10 μM), pemetrexed (1 μM) alone or in combination for 24 hr. (*c*) *TRIB*3 qPCR in adenocarcinoma A549 lung cancer cell lines treated with ABTL0812 (30 μM), cisplatin (10 μM), pemetrexed (1 μM) alone or in combination for 24 hr. Data represent mean ± SD, $n = 3$. ****$p < 0.0001$ by ANOVA with Sidak *post hoc* multiple comparison test. (*d*) Tumor growth of subcutaneously implanted adenocarcinoma A549 lung cancer cells in nude mice treated with vehicle ($n = 7$), cisplatin/pemetrexed ($n = 20$; 2/100 mg/kg) or a combination of ABTL0812 (120 mg/kg) with cisplatin/pemetrexed ($n = 20$; 2/100 mg/kg) for 35 days. The data are expressed as tumor volume increment using treatment Day 0 volumes as a reference. Data represent mean ± SD, $n = 5$. *$p < 0.1$, ***$p < 0.001$, &&, by ANOVA with Sidak *post hoc* multiple comparison test. (*e*) Representative images showing TRIB3 staining in the adenocarcinoma A549 lung cancer cells derived tumors treated with cisplatin/pemetrexed (2/100 mg/kg) or a combination of ABTL0812 with cisplatin/pemetrexed for 35 days. Scale bar

100 µm. Graph represents TRIB3 quantification as percentage of positive area (upper Graph) and intensity (lower graph).